

Supplementary Information for

Structural basis of undecaprenyl phosphate glycosylation leading to polymyxin resistance in Gram-negative bacteria

Khuram U Ashraf^{1,2}, Mariana Bunoro-Batista^{3,*}, T. Bertie Ansell^{4,&*}, Ankita Punetha^{1,2,*}, Stephannie Rosario-Garrido^{1,2}, Emre Firlar^{5,#}, Jason T. Kaelber⁵, Phillip J. Stansfeld³, Vasileios I. Petrou^{1,2,†}

¹Department of Microbiology, Biochemistry, and Molecular Genetics, New Jersey Medical School, Rutgers Biomedical Health Sciences, Newark, NJ, USA

²Center for Immunity and Inflammation, New Jersey Medical School, Rutgers Biomedical Health Sciences, Newark, NJ, USA

³School of Life Sciences and Department of Chemistry, University of Warwick, Coventry, United Kingdom

⁴Department of Biochemistry, University of Oxford, Oxford, United Kingdom

⁵Rutgers Cryo-EM & Nanoimaging Facility, Rutgers, the State University of New Jersey, Piscataway, NJ, USA

*M.B.-B., T.B.A., and A.P. contributed equally

&Current affiliation: Division of Cryo-EM and Bioimaging, SLAC National Accelerator Laboratory, CA, USA

#Current affiliation: Bristol Myers Squibb, Discovery and Development Sciences, Lawrenceville, NJ

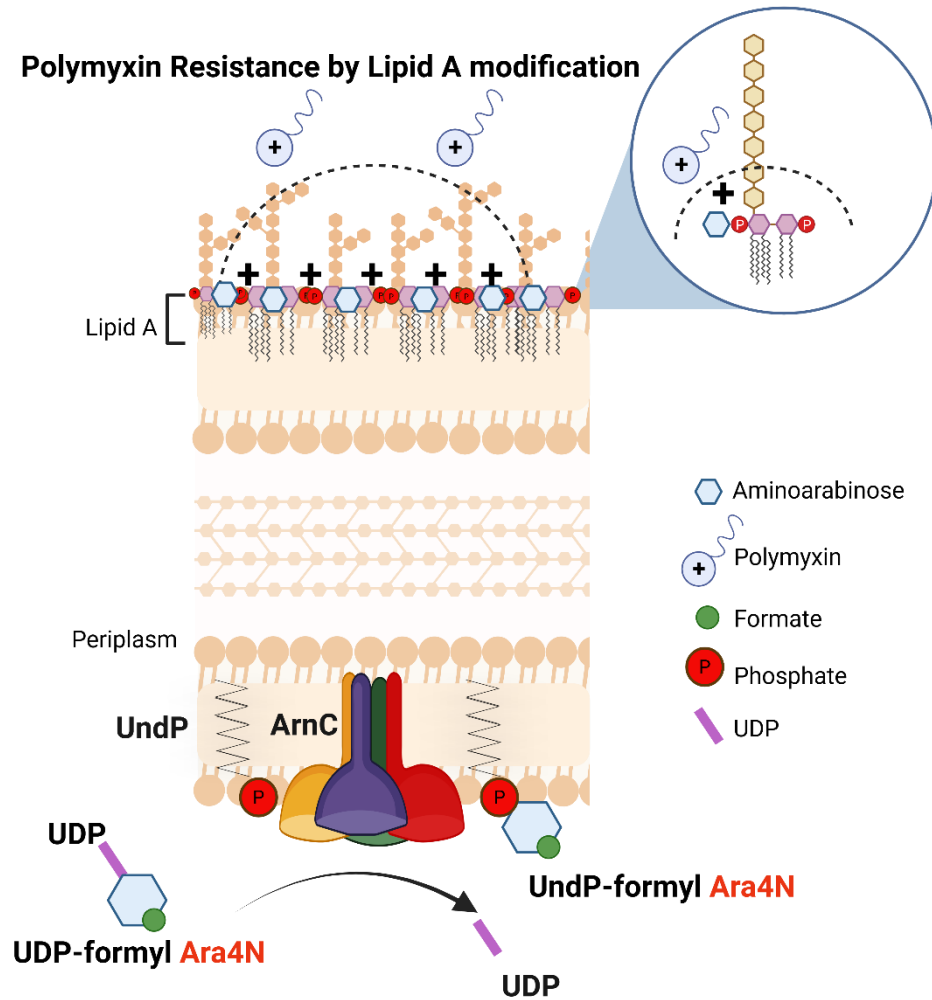
†Correspondence should be addressed to: vasileios.petrou@rutgers.edu (V.I.P.)

Supplementary Information includes:

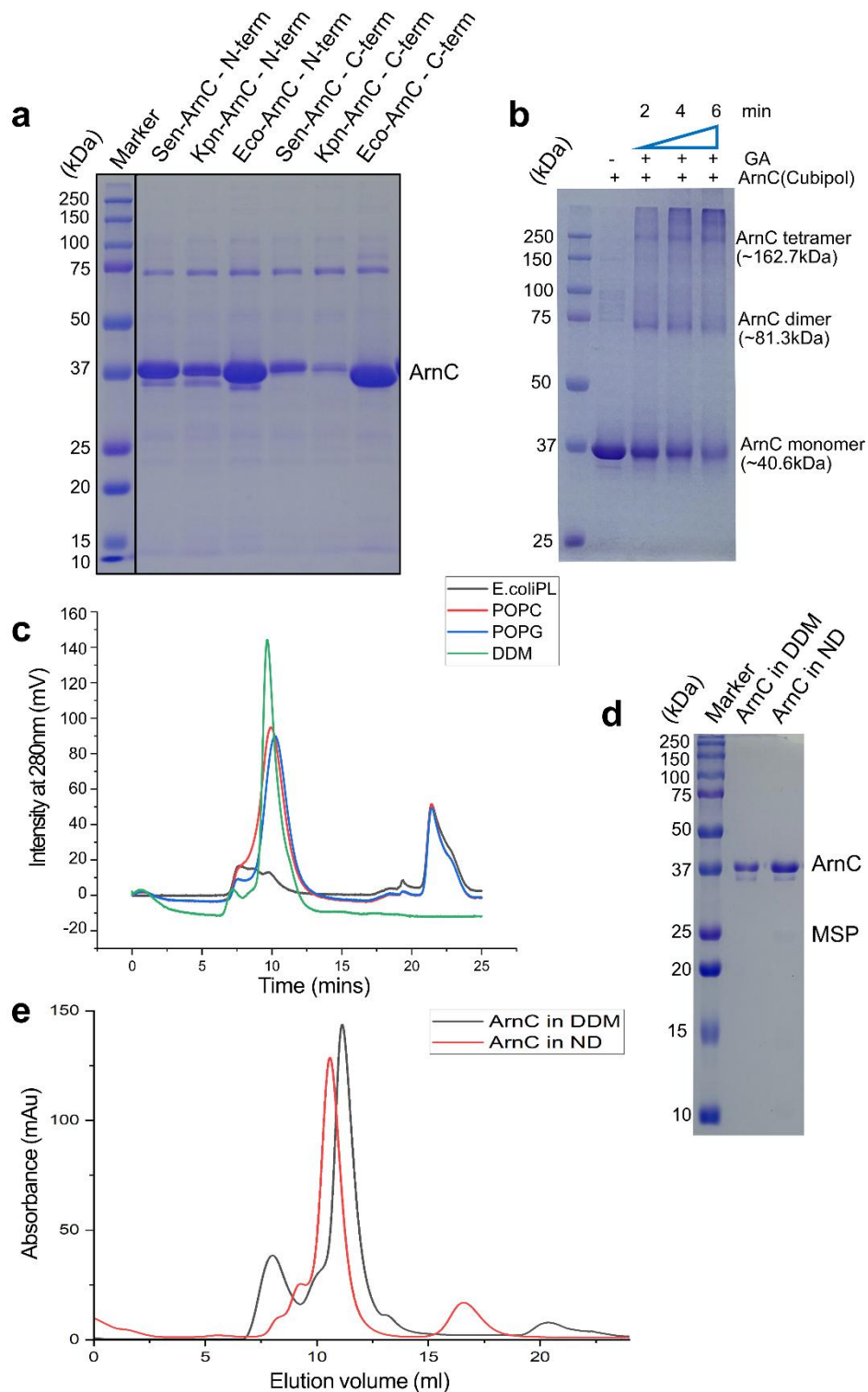
Supplementary Figure 1-17

Supplementary Table 1-3

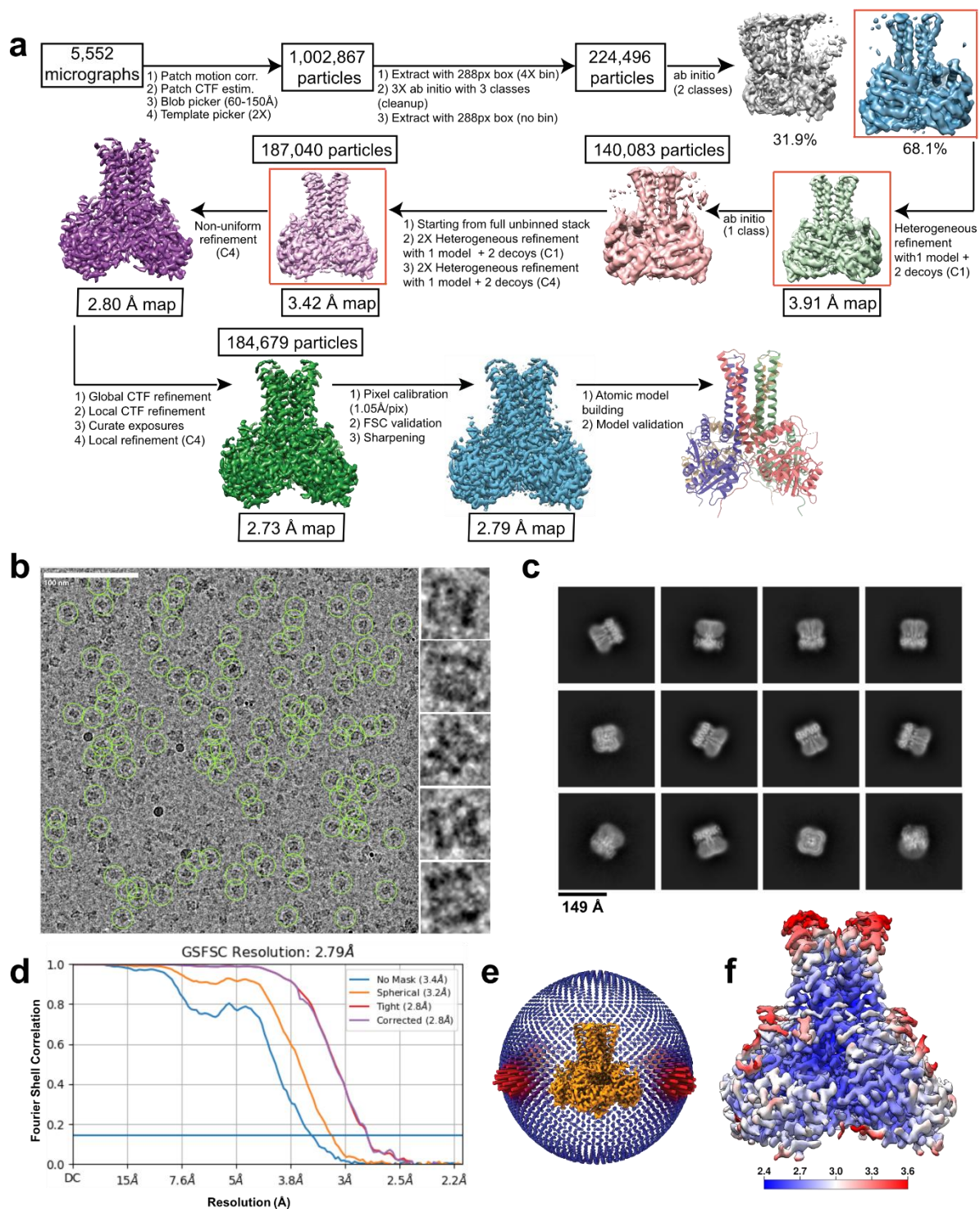
Polymyxin Resistance by Lipid A modification



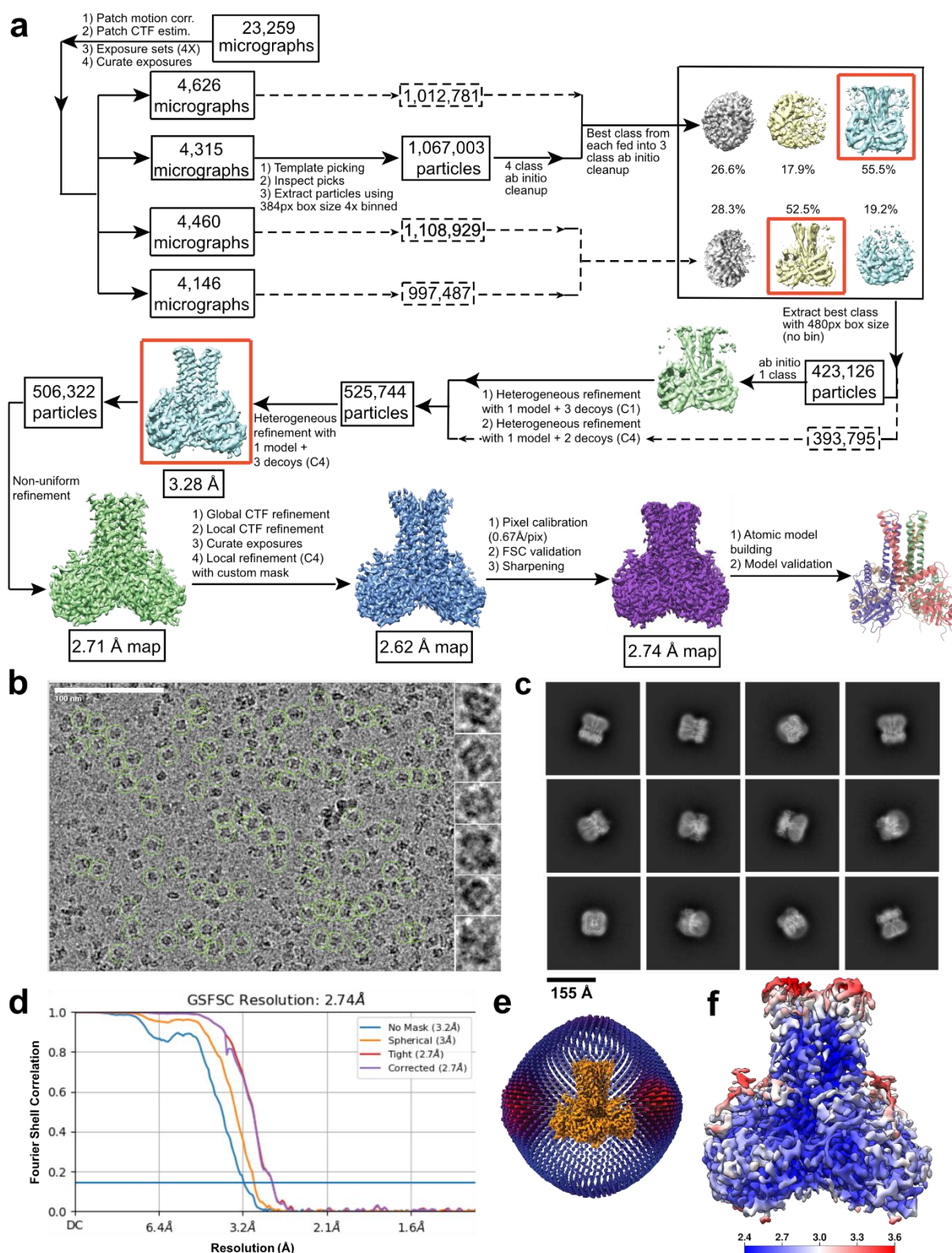
Supplementary Fig. 1. The ArnC enzyme linked to polymyxin resistance. Schematic representation of the ArnC enzyme in the inner membrane of Gram-negative bacteria and the chemical reaction it catalyzes. The aminoarabinose sugar after its association with UndP is ultimately used to decorate the phosphates of Lipid A, reducing the negative charge of the outer bacterial membrane, and leading to polymyxin resistance. Created in Biorender. Rosario, S. (2025) [<https://BioRender.com/x4gz6oc>]



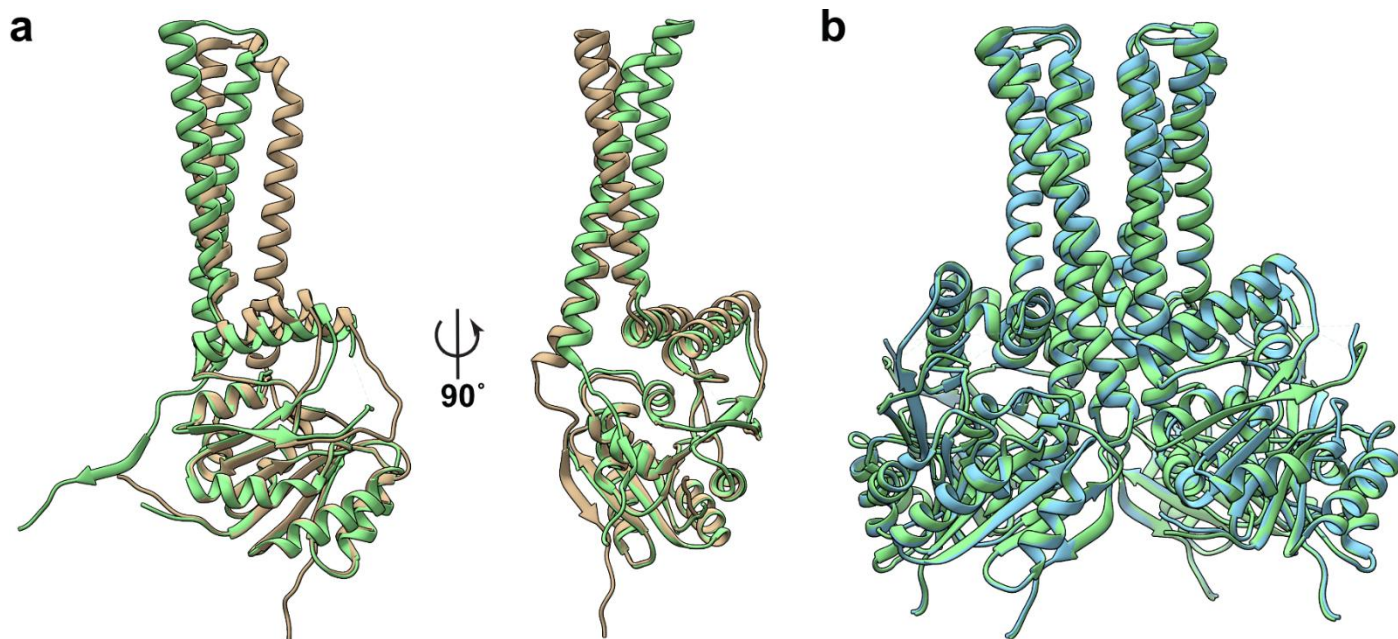
Supplementary Fig. 2. Expression, purification and nanodisc reconstitution of *S. enterica* ArnC. **a)** SDS-PAGE gel showing relative expression of ArnCs from *Salmonella enterica* (Sen), *Klebsiella pneumoniae* (Kpn) and *Escherichia coli* (Eco), with either N-terminal or C-terminal expression tags. **b)** SDS-PAGE gel showing extraction of *S. enterica* ArnC using Cubipol polymer and glutaraldehyde (GA) treatment for the indicated times. Bands for a monomer, dimer and tetramer are observed. **c)** Size-exclusion chromatography elution profiles of DDM-solubilized ArnC from *S. enterica*, and MSP1E3D1 nanodisc reconstituted samples (after bio-bead removal) using either POPC, POPG or *E. coli* polar lipid (E.coliPL) for reconstitution. Profiles were obtained using a Superdex 200 Increase 5/150 GL column (Cytiva). **d)** SDS-PAGE gel of ArnC from *S. enterica* large-scale purification, showing ArnC in DDM after affinity purification, and ArnC reconstituted into MSP1E3D1/POPG nanodiscs (ND). **e)** Size-exclusion chromatography elution profiles of purified ArnC in detergent (black), and incorporated into a nanodisc (red), on a Superdex 200 Increase 10/300 GL column (Cytiva).



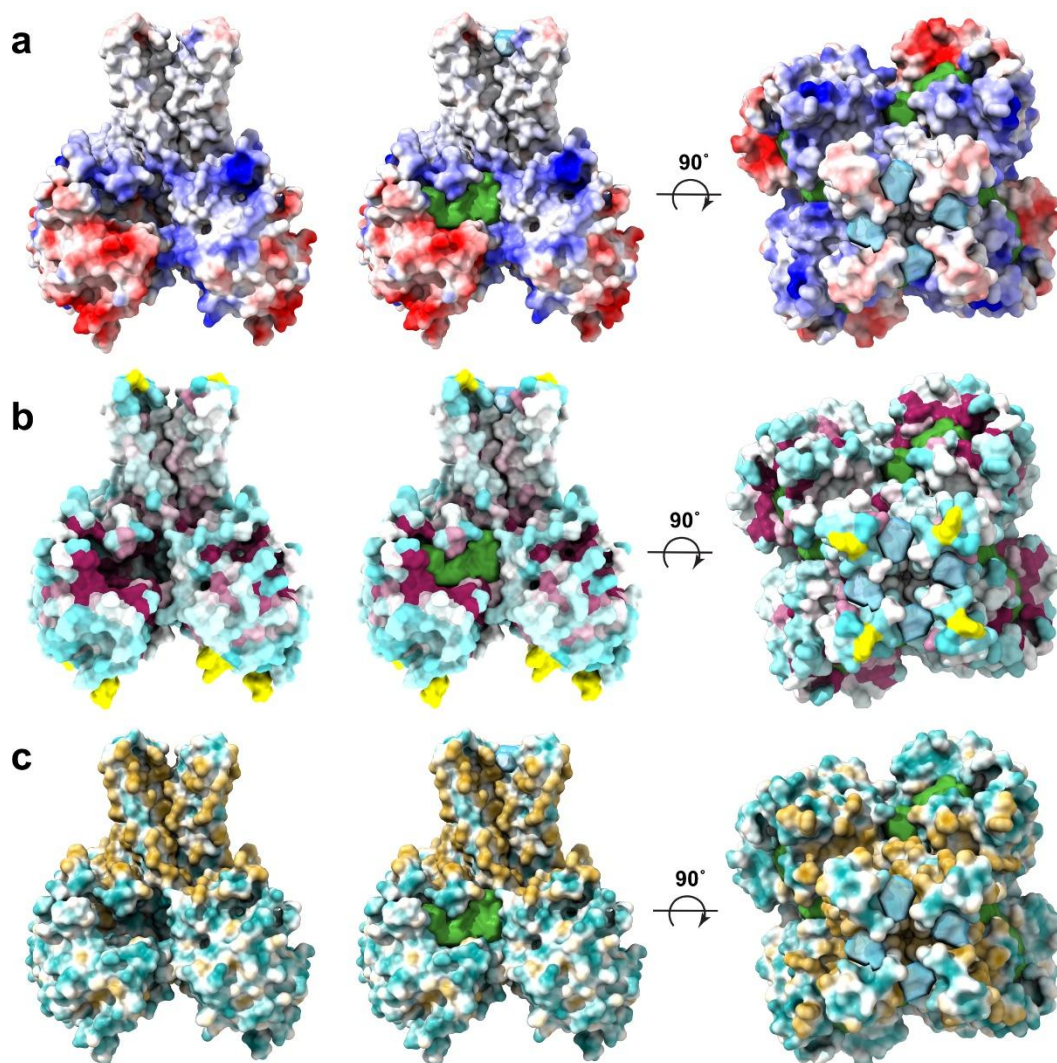
Supplementary Fig. 3. Cryo-EM analysis of apo ArnC_{se} collected on Talos Arctica. **a)** Data processing workflow used to determine the structure of nanodisc-reconstituted ArnC_{se} from a Talos Arctica dataset. **b)** Representative electron micrograph of nanodisc-reconstituted ArnC_{se} from Talos Arctica. Particles included in the final reconstruction are marked with green circles. Insets on the right show individual single particles from the micrograph. Scale bar, 100nm. **c)** Representative 2D class averages after reference-free 2D classification of the final particle stack in cryoSPARC. **d)** Fourier shell correlation (FSC) curve for apo nanodisc-reconstituted ArnC_{se} after the final local refinement in cryoSPARC. **e)** Euler angle distribution plot of all ArnC_{se} particles used in the final reconstruction. Final map shown in orange. Each orientation is represented by a cylinder, with each cylinder's height and color (from blue to red) proportional to the number of particles for that specific orientation. **f)** Local resolution map for the final ArnC_{se} reconstruction. Local resolution was estimated using an implementation of the blocres program in cryoSPARC. Coloring shown from deep blue (2.4 Å) to red (≥ 3.6 Å).



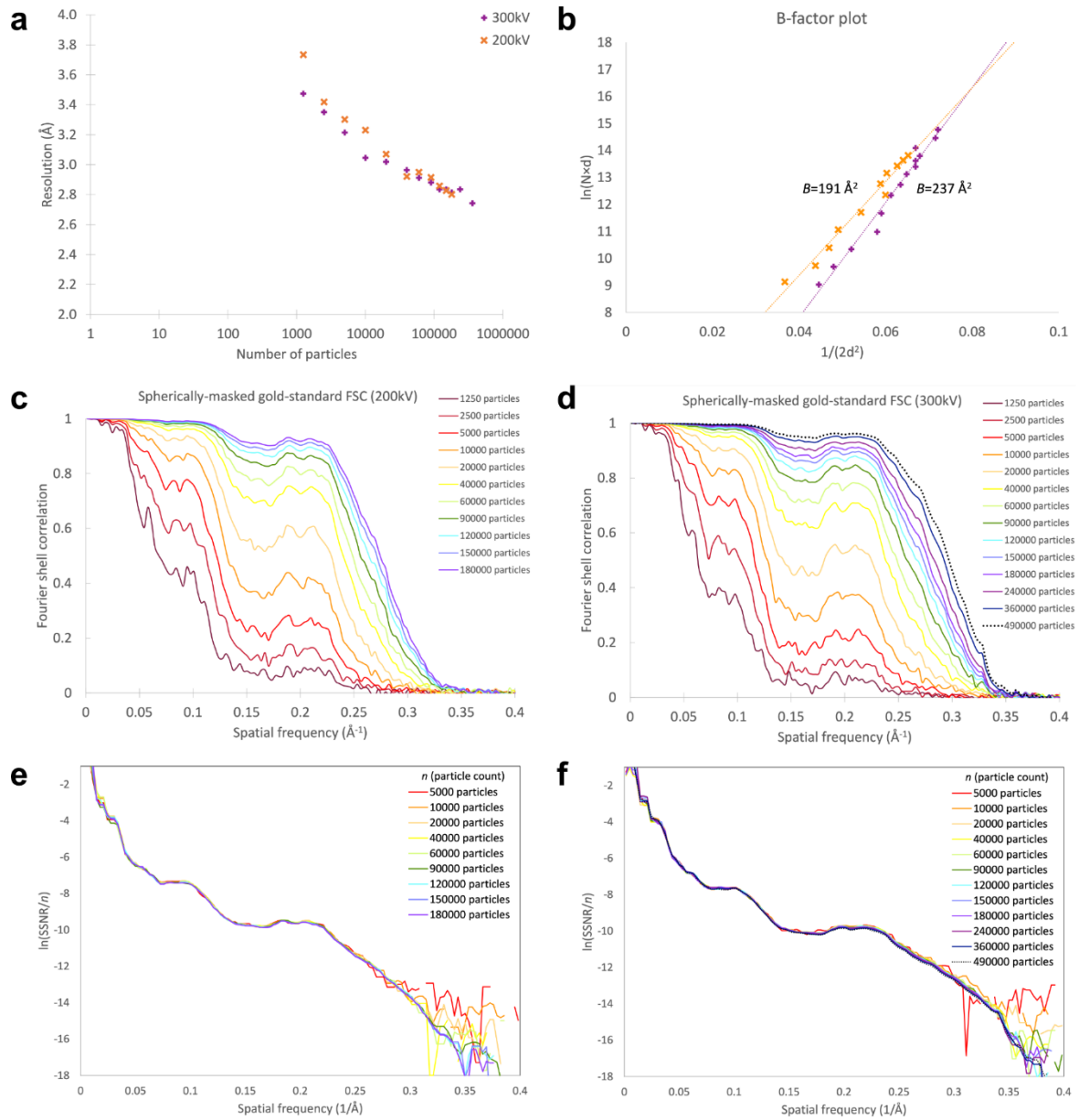
Supplementary Fig. 4. Cryo-EM analysis of apo ArnC_{se} collected on Titan Krios. **a)** Data processing workflow used to determine the structure of nanodisc-reconstituted ArnC_{se} from a Krios microscope dataset. **b)** Representative electron micrograph of ArnC_{se} from Titan Krios. Particles included in the final reconstruction are marked with green circles. Insets on the right show individual single particles from the micrograph. Scale bar, 100nm. **c)** Representative 2D class averages after reference-free 2D classification of the final particle stack in cryoSPARC. **d)** Fourier shell correlation (FSC) curve for apo nanodisc-reconstituted ArnC_{se} after the final local refinement in cryoSPARC. **e)** Euler angle distribution plot of all ArnC_{se} particles used in the final reconstruction. Final map shown in orange. **f)** Local resolution map for the final ArnC_{se} reconstruction. Coloring shown from deep blue (2.4 Å) to red (≥3.6 Å).



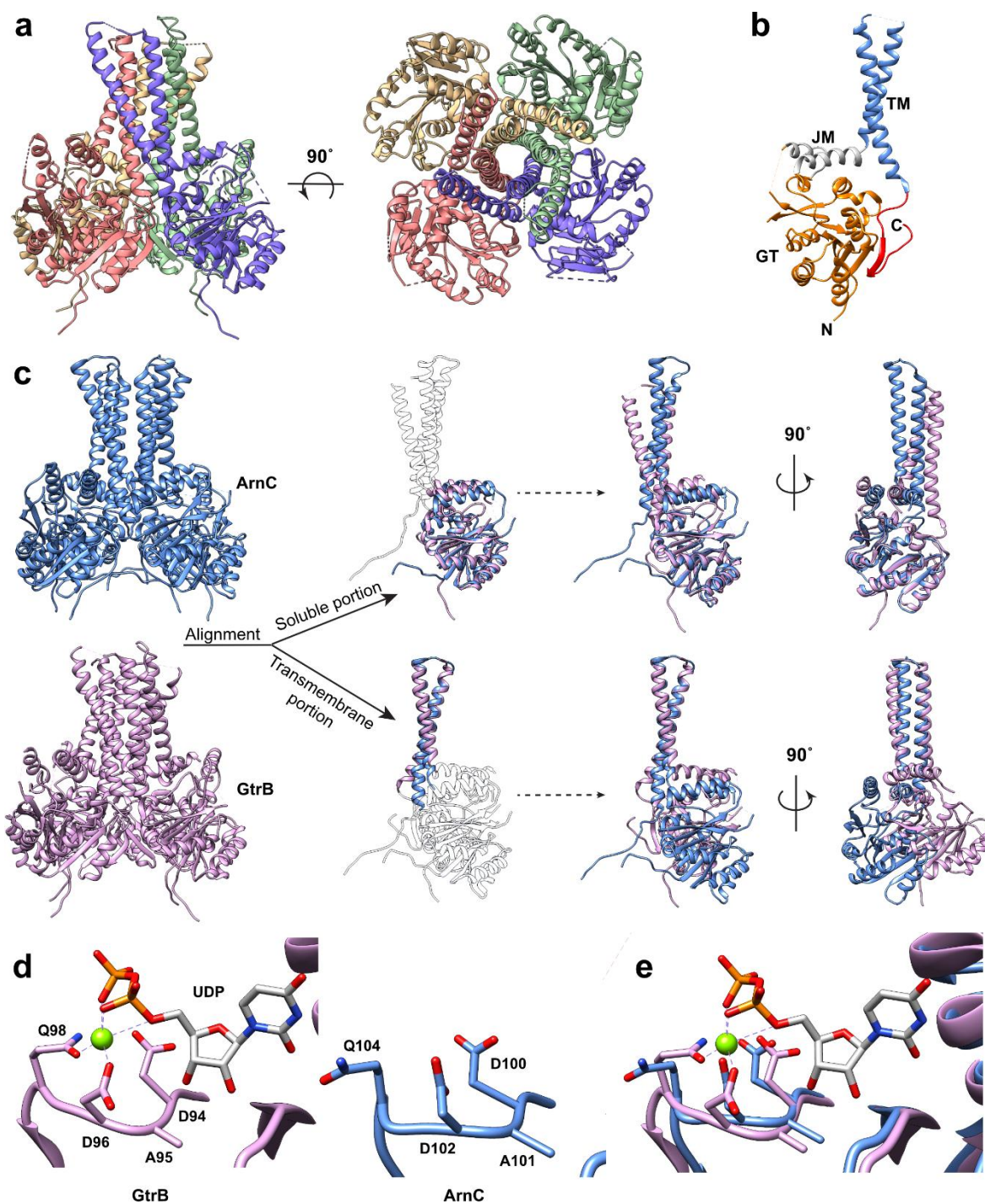
Supplementary Fig. 5. apo ArnC model comparison. **a)** Comparison between the final apo ArnC_{Se} atomic model (green) and the AlphaFold predicted atomic model of ArnC from *E. coli* (AF-P77757-F1-v4) used as a starting model for model building. RMSD between 312 atom pairs is 9.54Å. **b)** Comparison between the final apo ArnC_{Se} atomic model built based on the Arctica dataset map (green) and the one build based on the Krios dataset map (light blue). RMSD between 1248 atom pairs is 0.67Å.



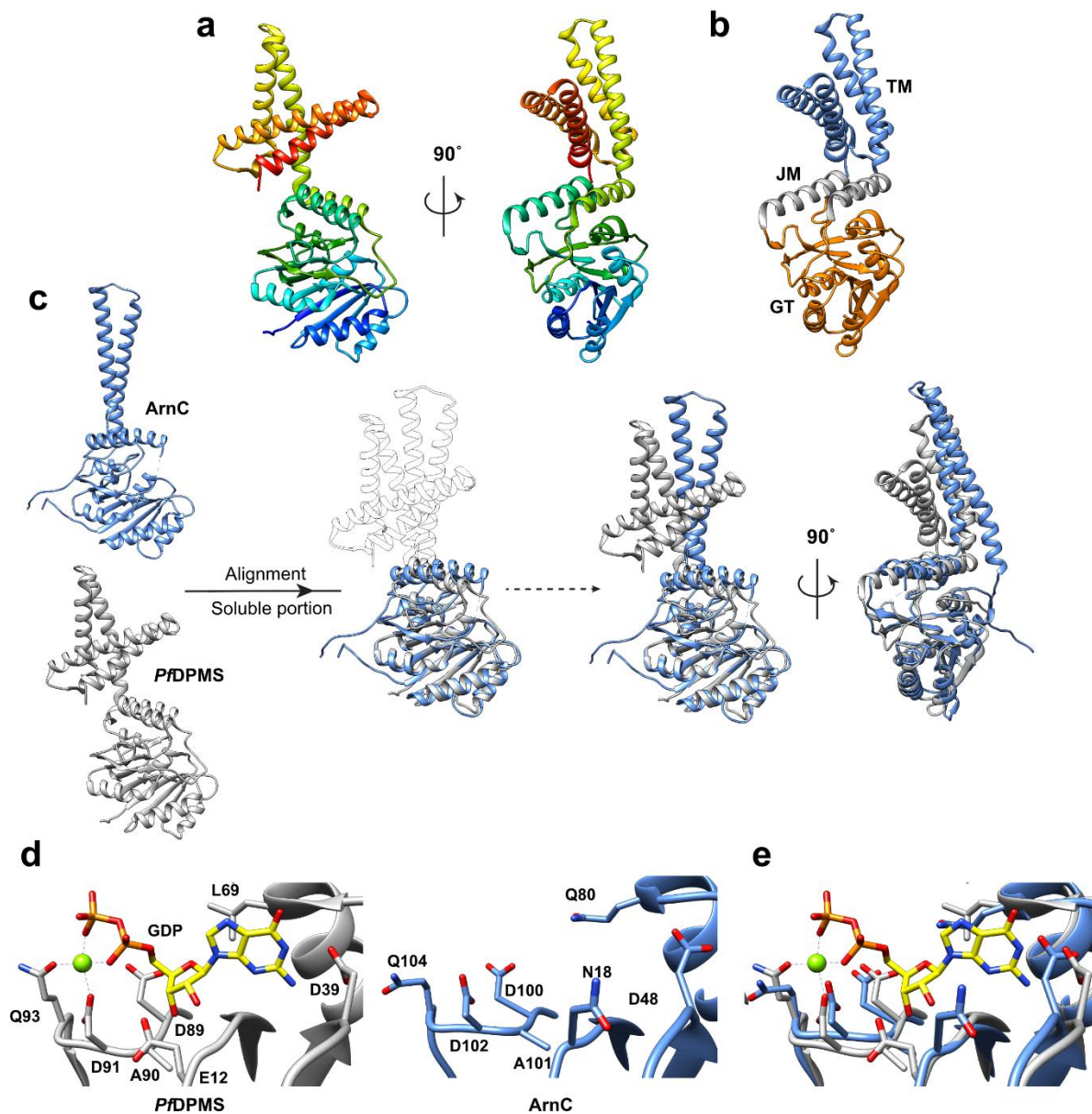
Supplementary Fig. 6. Physicochemical properties of ArnC. a) ArnC_{Se} rendered in surface representation colored by electrostatic potential. b) ArnC_{Se} surface colored by residue conservation on a yellow/white (no conservation) to purple (absolute conservation) scale. c) ArnC_{Se} surface colored by Wimley-White hydrophobicity, on a cyan (very hydrophilic) to gold (very hydrophobic) scale. Two orthogonal views are presented with cavities shown either empty (left) or filled with a green (cavity 1) or light blue (cavity 2) volume.



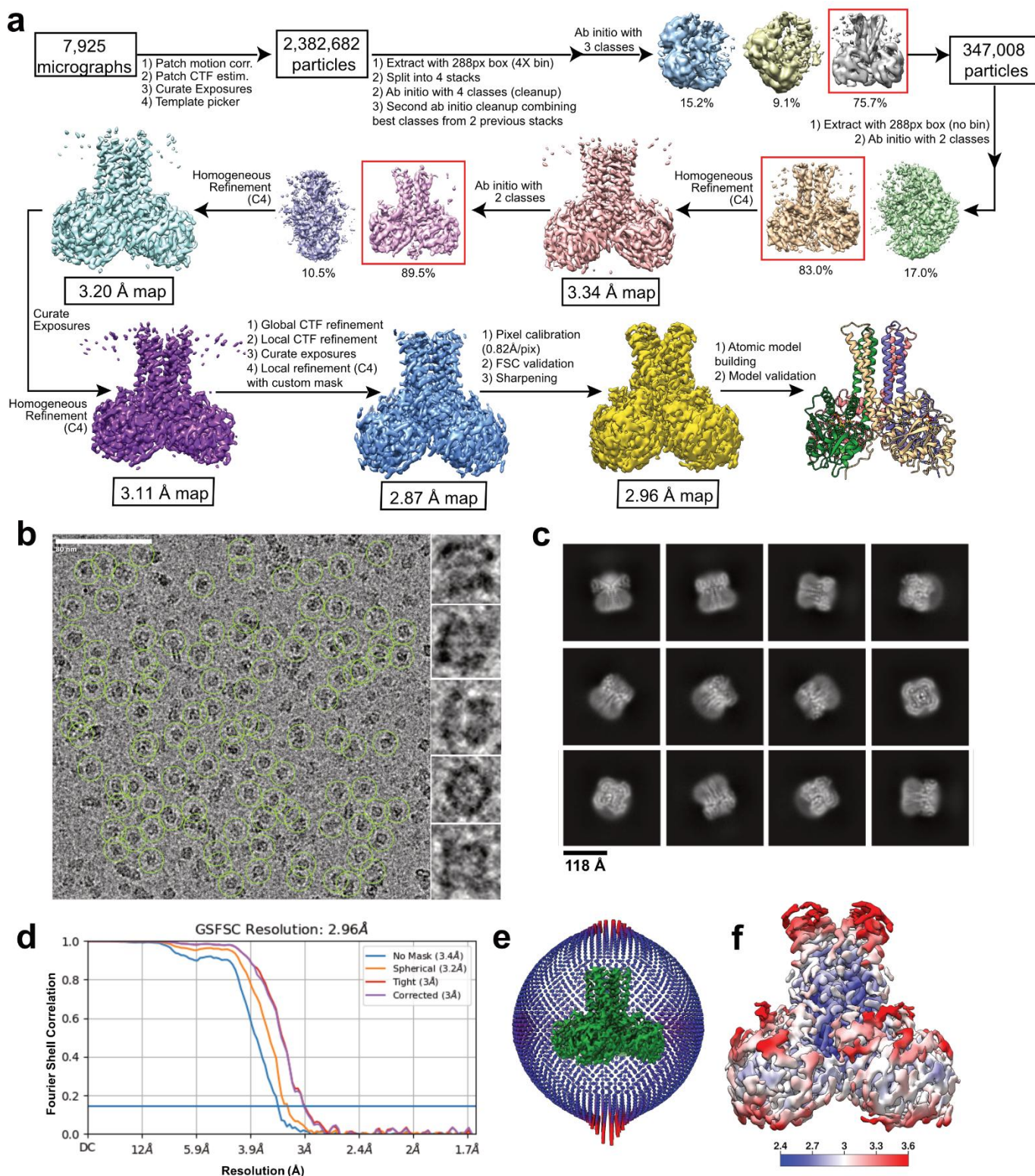
Supplementary Fig. 7. Effect of particle count on reconstructed information for apo ArnC. **a**) Resolution vs. number of particles for the dataset acquired with a 200 kV TEM (orange) and 300 kV TEM (purple). **b**) Transform of that data into a B-factor plot showing the natural log of the number of particles (N) multiplied by the resolution (d) plotted as a function of $1/2d^2$; colors as panel A. The slope of the B-factor plot represents the resolution-dependent signal dampening and is analogous to the crystallographic temperature factor. **c, d**) Spherically-masked gold-standard Fourier shell correlation between even-odd half-maps reconstructed with halves of the data subsets from data acquired at 200 kV (C) and 300 kV (D); colored by the total number of particles in the subset (i.e. both halves). **e, f**) Transform of that data into a “universal plot” for 200 kV (E) and 300 kV (F) datasets by dividing the Fourier shell correlation from panels (C) and (D) by the particle count and log-transforming. The “universal plots” illustrate the information content per particle.



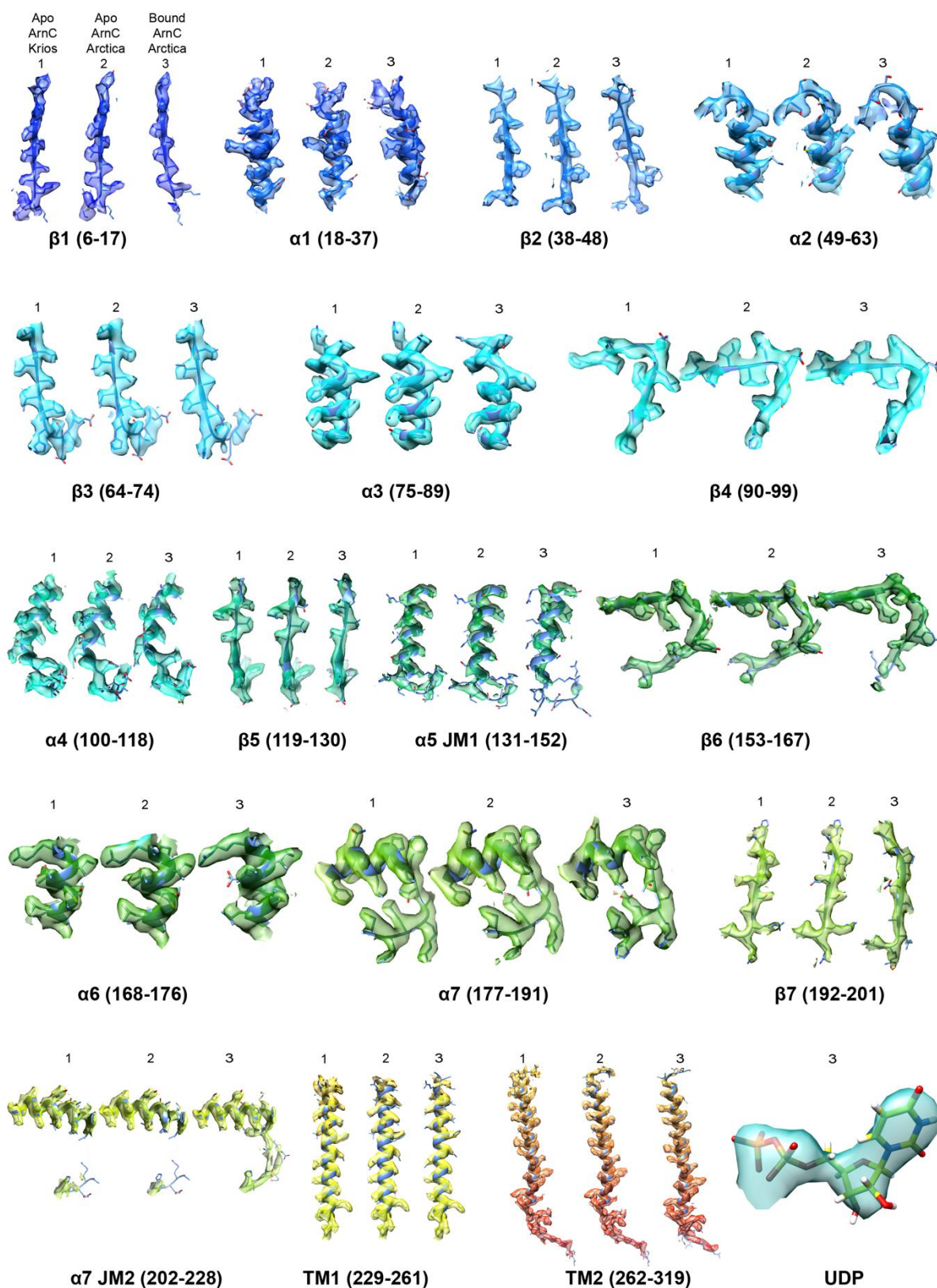
Supplementary Fig. 8. Comparison with the glycosyltransferase GtrB. **a**) Crystal structure of GtrB (PDB 5EKP) in ribbon representation with per protomer coloring. **b**) A single GtrB protomer is comprised of a GT-A fold glycosyltransferase domain (orange), two amphipathic juxtamembrane (JM) helices (gray), two transmembrane (TM) helices (blue) and a C-terminal β -hairpin (red). **c**) Comparison of ArnC (blue) and GtrB (pink), with a single protomer from each structure aligned via the GT-A soluble domain or the transmembrane domain. **d**) Comparison of the signature metal-coordinating DXD motif from GtrB (left) and *apo* ArnC (right). **e**) Superposition of the DXD motifs from GtrB and ArnC. Coloring as in (d).



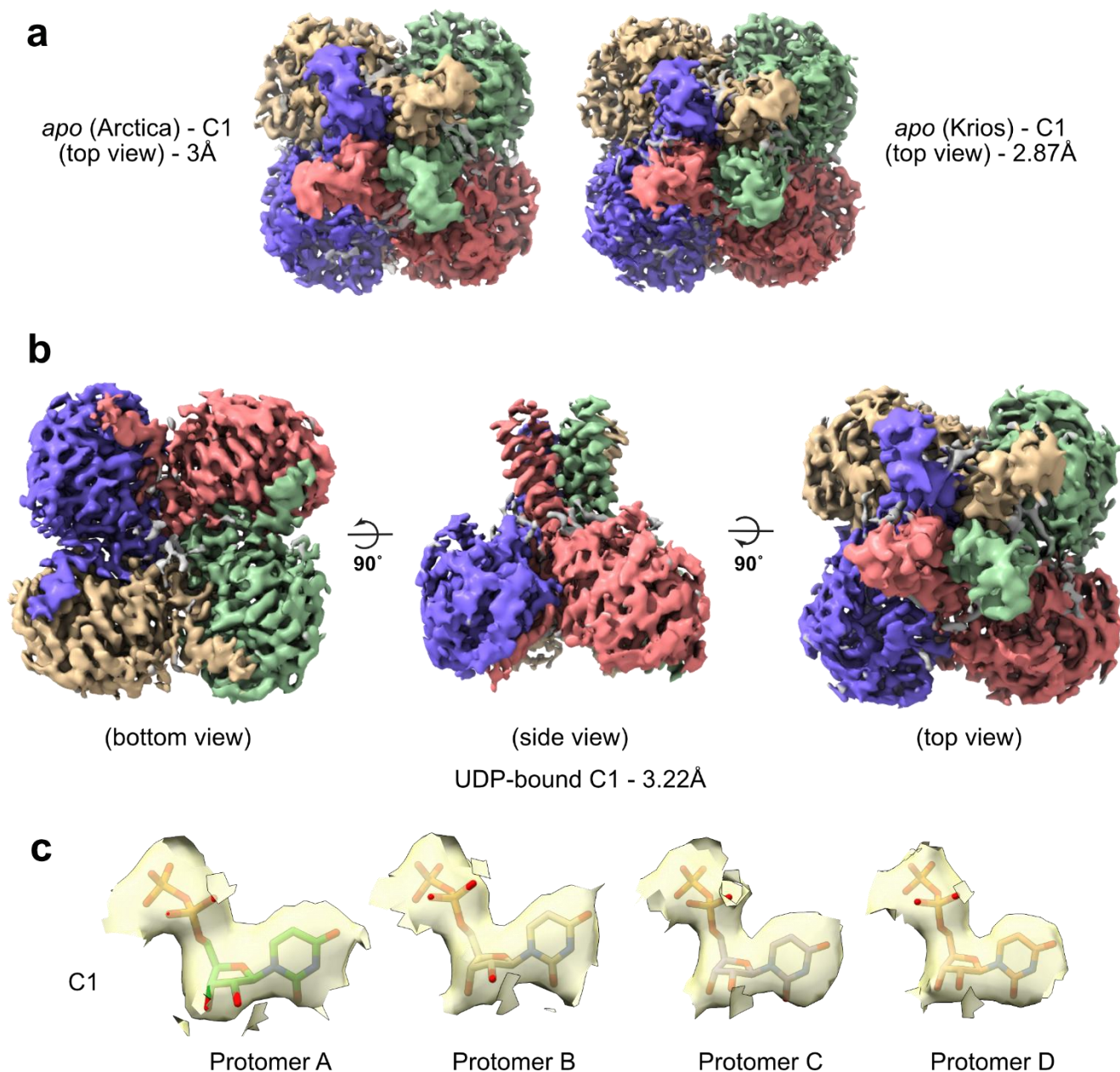
Supplementary Fig. 9. Comparison with *PDPMS*. **a**) Crystal structure of *Pyrococcus furiosus* DPMS (PDB 5MLZ) drawn in ribbon representation with rainbow coloring from N-terminus (blue) to C-terminus (red). Two orthogonal views are shown. **b**) DPMS is comprised of a GT-A fold GT domain (orange), two amphipathic juxtamembrane (JM) helices (gray), and four transmembrane (TM) helices (blue). **c**) Comparison of ArnC (blue) and DPMS (gray), with a single protomer of ArnC aligned with DPMS via the GT-A soluble domain. **d**) Comparison of the signature metal-coordinating DXD motif from DPMS (left) and *apo* ArnC (right). **e**) Superposition of the DXD motifs from DPMS and ArnC. Coloring as in (d).



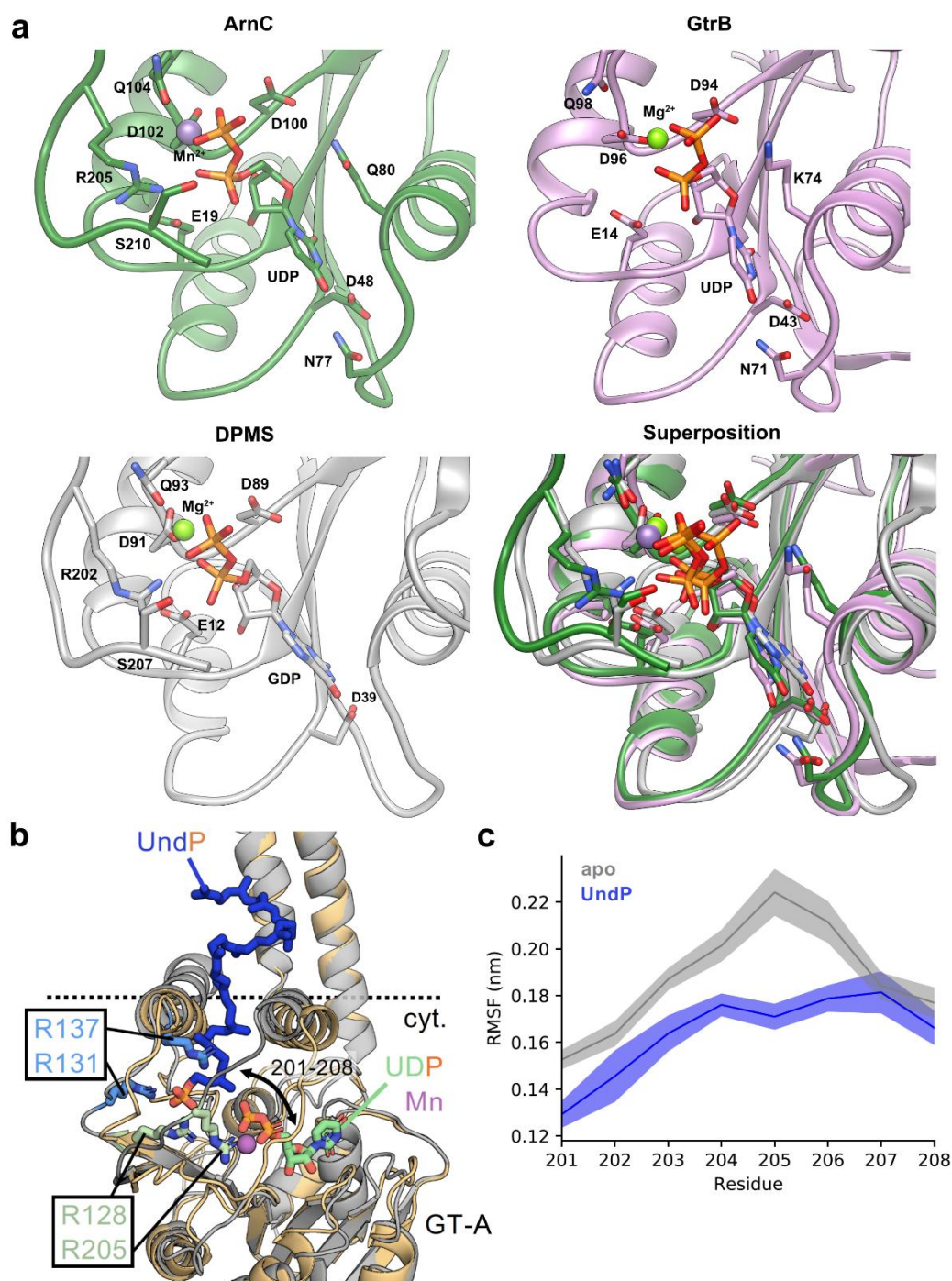
Supplementary Fig. 10. Cryo-EM analysis of UDP-bound ArnC_{Se} collected on Talos Arctica. **a)** Data processing workflow used to determine the structure of nanodisc-reconstituted UDP-bound ArnC_{Se} from the dataset collected on a Talos Arctica microscope. **b)** Representative electron micrograph of UDP-bound ArnC_{Se} from Talos Arctica. Particles included in the final reconstruction are marked with green circles. Insets on the right show individual single particles from the micrograph. Scale bar, 80nm. **c)** Representative 2D class averages after reference-free 2D classification of the final particle stack in cryoSPARC. **d)** Fourier shell correlation (FSC) curve for UDP-bound nanodisc-reconstituted ArnC_{Se} after the final local refinement in cryoSPARC. **e)** Euler angle distribution plot of all UDP-bound ArnC_{Se} particles used in the final reconstruction. Final map shown in green. **f)** Local resolution map for the final UDP-bound ArnC_{Se} reconstruction. Coloring shown from deep blue (2.4 Å) to red (≥3.6 Å).



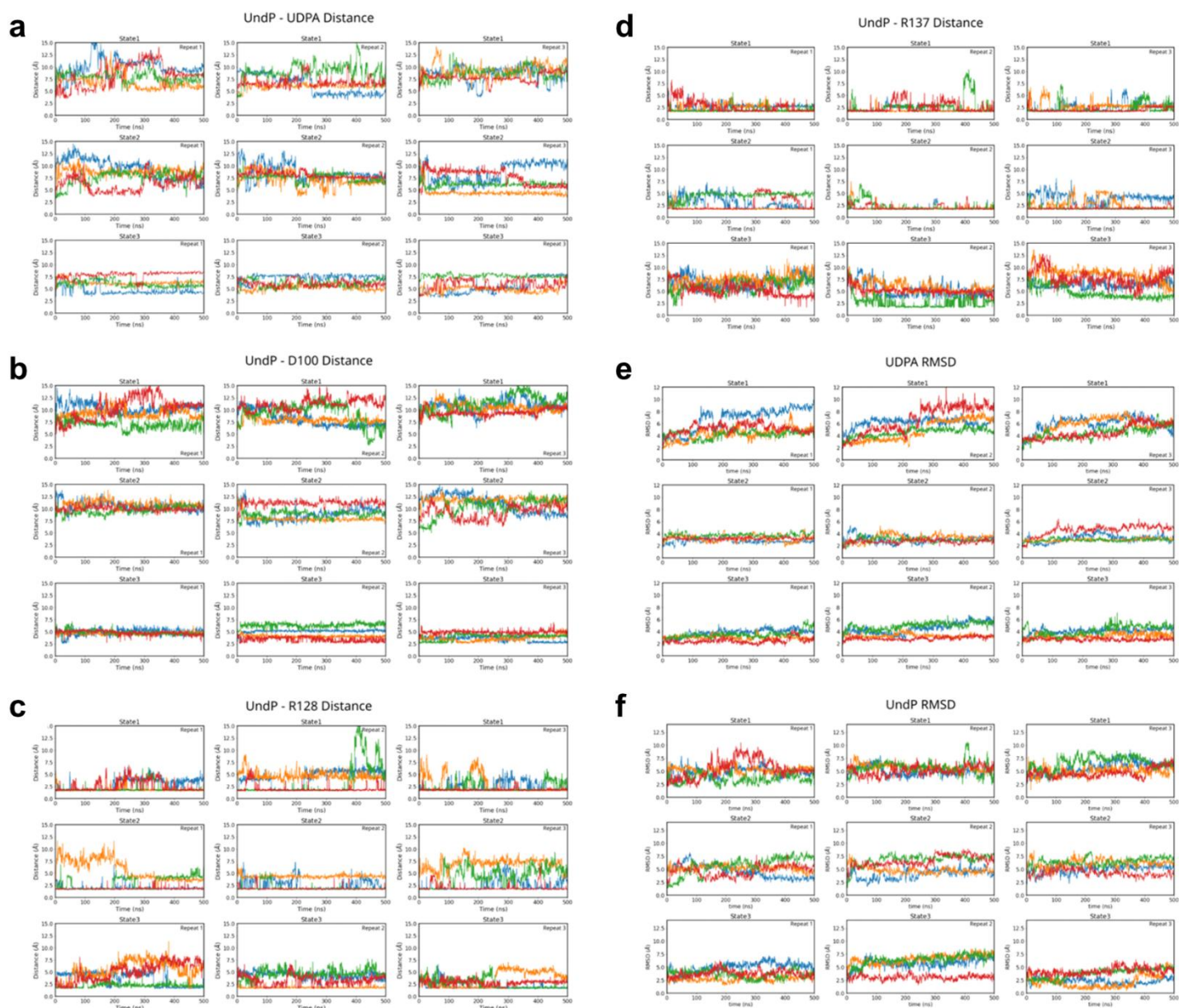
Supplementary Fig. 11. Cryo-EM densities of ArnC reconstructions. Cryo-EM densities in surface representation are superimposed on ArnC models for each of the three datasets as indicated: apo ArnC – Krios dataset (left), apo ArnC – Arctica dataset (middle), and UDP-bound ArnC – Arctica dataset (right). Coloring of densities is in rainbow from N-terminus (blue) to C-terminus (red). UDP (green) is shown as sticks.



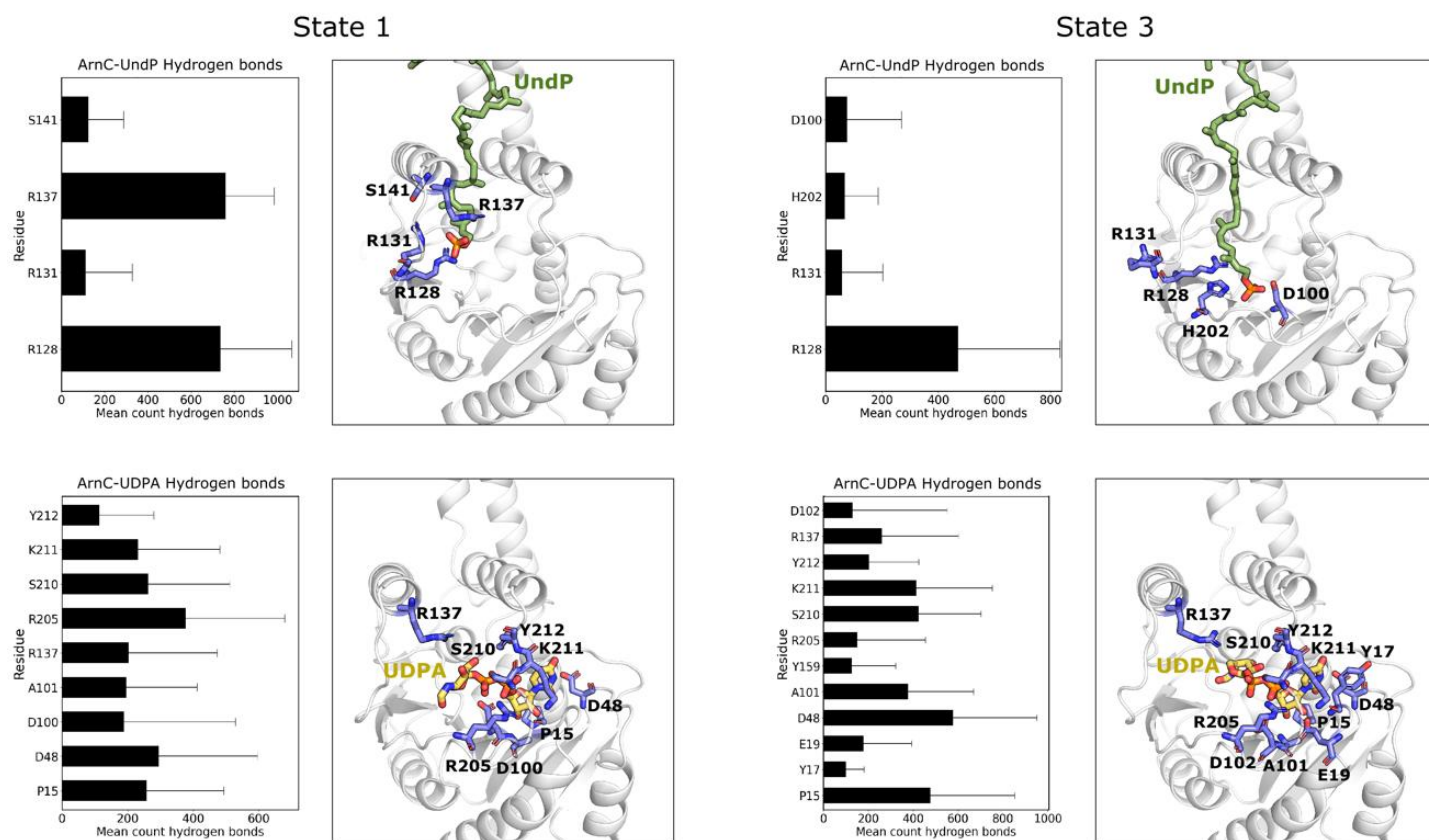
Supplementary Fig. 12. ArnC reconstructions without symmetry (C1). **a)** Reconstructions of the final particle stacks from the *apo* (Arctica) and *apo* (Krios) datasets without imposing any symmetry. Top-down views are presented. **b)** Reconstruction of the final particle stack of the UDP-bound dataset without imposing any symmetry. Three orthogonal views are presented. Coloring for (a) and (b) is per subunit. **c)** Densities corresponding to the UDP nucleotide in each of the four protomers of ArnC from the reconstruction shown in (b). Densities appear very similar even in the absence of imposed fourfold symmetry.



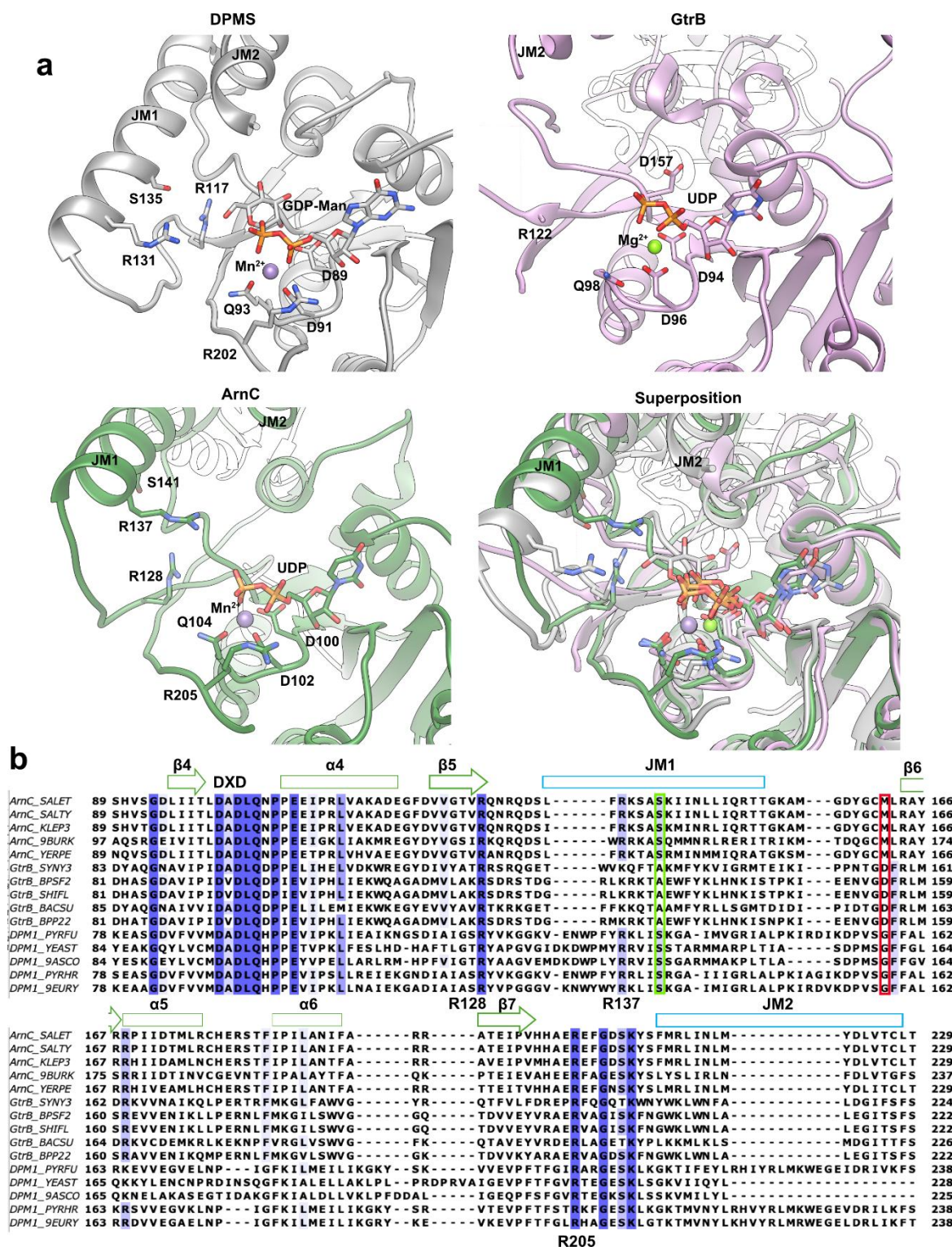
Supplementary Fig. 13. Substrate binding in ArnC. **a**) Comparison of nucleotide binding between the UDP-bound ArnC structure, GtrB (PDB 5EKP) and DPMS (PDB 5MLZ). Side chains for residues likely contributing to substrate binding (within 5Å of the nucleotide or the metal) are shown as sticks. Mn^{2+} is shown as a purple sphere and Mg^{2+} is shown as a green sphere. The superposition indicates the overlapping coordination of the nucleotide in all three enzymes. **b**) Snapshot of the final UndP binding pose within the ArnC GT-A domain from atomistic MD simulations (ArnC: gray, UndP: blue) overlaid with the ArnC-UDP structure (ArnC: light orange, UDP: green). UndP and UDP are shown as sticks and phosphate groups are colored orange. The Mn^{2+} ion is shown in purple. Arginine residues coordinating the UndP in simulations are shown in blue. Additional arginine residues facing the UDP site, and which may therefore be involved in coordination of incoming nucleotides, are shown in mint. UndP and UDP can both be coordinated within the GT-A domain without coordination clashes. The position of a flexible loop (residues 201-208) is indicated. **c**) Stabilization of the flexible loop by UndP. Mean root mean square fluctuation (RMSF) of the loop indicated in a across 3 x 100 ns atomistic simulations of ArnC with UndP bound to one GT-A domain (blue) compared to the three remaining apo GT-A domains (gray). Error bars represent standard error of the mean (SEM).



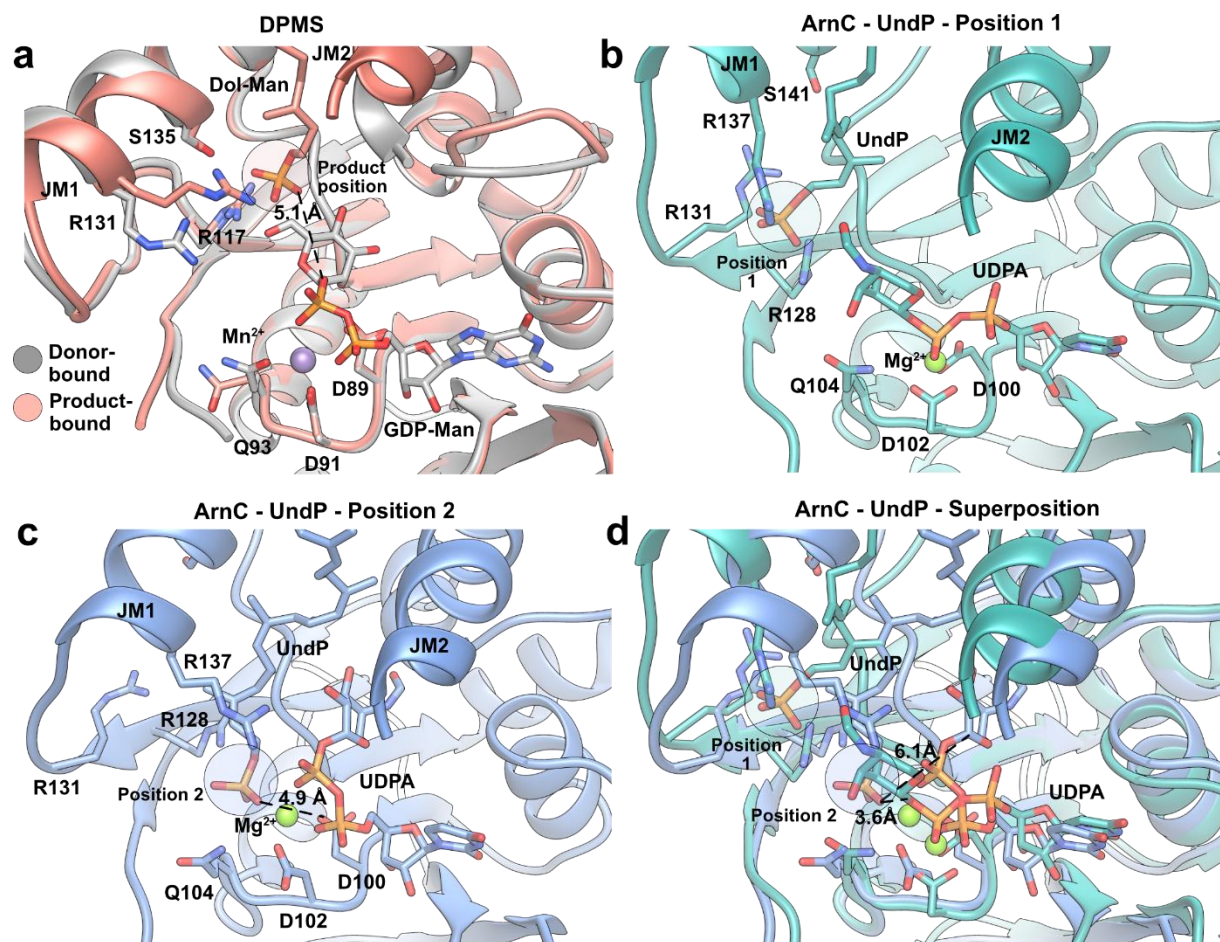
Supplementary Fig. 14. Atomistic simulations of substrate-bound ArnC. Time traces of (a) UndP–UDPa, (b) UndP–D100, (c) UndP–R128 and (d) UndP–R137 distances, as well as (e) UDPa and (f) UndP RMSDs. Each color represents a different subunit of the tetramer. Traces are shown for each state and replicate.



Supplementary Fig. 15. Hydrogen bonds between ArnC and its substrates. For each state, hydrogen bonds with undecaprenyl phosphate (UndP) (top) and UDP-L-Ara4FN (UDPA) (bottom) are shown. In state 1, the conserved arginines R128 and R137 coordinate the phosphate group of UndP, however, for state 3, only R128 contributes in the coordination of the lipid. Although the initial configuration for UDP-L-Ara4FN (UDPA) is different for state 1 and 3, its interaction with ArnC is similar for both states, due to the reorientation that the sugar group undergoes in state 1. Hydrogen bonds between the Ara4FN group and the conserved arginine R137 stabilize the sugar group for both states.



Supplementary Fig. 16. Catalytic residues in the ArnC, GtrB and DPMS families. **a)** Potential catalytic residues for DPMS (PDB 5MM0) (top left), and GtrB (PDB 5KEP) (top right), and their equivalent residues (based on position and conservation) in ArnC in the UDP-bound state (bottom left). A superposition of all three is shown in bottom right. Mn^{2+} shown as purple sphere, and Mg^{2+} shown as green sphere. The nucleotides (GDP-Man and UDP) are color matched to each structure with the phosphates shown in orange. **b)** Sequence alignment between $\beta 4$ and JM1 of the GT-A domain from representative species of the ArnC, GtrB and DPMS families. Highly conserved residues are highlighted in blue and partially conserved residues are shown in lighter blue. *Pf*DPMS S141 and its corresponding residues in ArnC (Ser) and GtrB (Ala) families are highlighted by a green box. GtrB D157 and its corresponding residues in ArnC (Met) and DPMS (Gly) families are highlighted by a red box. The DXD motif and ArnC residues R128, R137 and R205 are marked on the alignment.



Supplementary Fig. 17. Coordination of the acceptor phosphate and catalysis in DPMS and ArnC. **a**) Superposition of the donor-bound *Pf*DPMS structure containing GDP-mannose (GDP-Man) (PDB 5MM0) and the product-bound *Pf*DPMS structure containing dolichol phosphate-mannose (Dol-Man) (PDB 5MM1). The mannose ring has been removed from the product-bound structure to showcase the position of the acceptor phosphate, which is highlighted with a red circle as the "Product position". The distance between the nearest O atom of the acceptor phosphate and the C1 of the mannose ring in the donor-bound structure is 5.1 Å. The Mn^{2+} of the donor-bound structure is shown as a purple sphere. **b**) Detail of the GT-A domain of ArnC from atomistic simulations corresponding to "State 1", showing the acceptor phosphate in "Position 1" coordinated by R128, R131, and R137. In this position, the C1 atom of the donor L-Ara4FN sugar (UDPA) is 7.7 Å away from the nearest O atom of the acceptor phosphate and is occluded by the rest of the sugar. **c**) Detail of the GT-A domain of ArnC from atomistic simulations corresponding to "State 3", showing the acceptor phosphate deeper into the GT-A domain in "Position 2", coordinated mainly by R128, Q104, D102. In this position, D100 is located 4.9 Å away from the acceptor phosphate. **d**) Superposition of ArnC from (b) and (c). The superposition shows the two positions for coordination of UndP and highlights the distances between the nearest O atom of the acceptor phosphate in position 2 with the C1 atom of the L-Ara4FN sugar (3.6 Å in "State 1", and 6.1 Å in "State 3"). The Mg^{2+} ion in panels (b)-(c) is shown as a green sphere.

Supplementary Table 1. Cryo-EM data collection, refinement, and validation statistics for *apo* ArnC (Krios), *apo* ArnC (Arctica) and ArnC:Mn:UDP complex structures.

Dataset	ArnC <i>apo</i> (Krios)	ArnC <i>apo</i> (Arctica)	ArnC:Mn:UDP (Arctica)
<i>PDB ID</i>	9B77	8VXH	9ASC
<i>EMDB ID</i>	EMD-44302	EMD-43617	EMD-43812
<i>EMPIAR ID</i>	EMPIAR-12002	EMPIAR-11924	EMPIAR-11987
Data collection and Processing			
<i>Microscope</i>	Titan Krios	Talos Arctica	Talos Arctica
<i>Camera</i>	Gatan K3	Gatan K2 Summit	Gatan K2 Summit
<i>Energy Filter</i>	Gatan BioQuantum (20eV)	Gatan BioQuantum (20eV)	Gatan BioQuantum (20eV)
<i>Magnification (nominal)</i>	130,000	130,000	165,000
<i>Voltage (kV)</i>	300	200	200
<i>Exposure time (s)</i>	1.2	7	5.3
<i>n frames</i>	40	35	53
<i>Dose rate (e-/pixel/s)</i>	19.969	5.420	5.034
<i>Electron exposure (e-/Å²)</i>	57.42	35.21	39.88
<i>Defocus range (μm)</i>	-0.8 to -2.0	-0.5 to -2.5	-0.5 to -2.5
<i>Nominal pixel size (Å)</i>	0.646	1.038	0.818
<i>Calibrated pixel size (Å)</i>	0.67	1.05	0.82
<i>Pixel size error (%)</i>	3.72	1.16	0.24
<i>Box size (pixels)</i>	480	288	288
<i>Symmetry imposed</i>	C4	C4	C4
<i>Micrographs collected (#)</i>	23,259	5,552	7,925
<i>Median per-frame motion (90% range) (Å)</i>	0.07 (0.05-0.44)	0.19 (0.11–0.64)	-
<i>Initial particle images (#)</i>	4,186,210	1,002,867	2,382,682
<i>Final micrographs (#)</i>	16,451	3,318	5,556
<i>Final particle images (#)</i>	490,807	184,679	216,104
<i>Map resolution (Å)</i>	2.74	2.79	2.96
<i>FSC threshold</i>	0.143	0.143	0.143
<i>Local map resolution range (Å)</i>	2.33-6.98	2.34-7.16	2.53-6.97
<i>Local map FSC threshold</i>	0.5	0.5	0.5
<i>3DFSC Sphericity</i>	0.982	0.971	0.967
Refinement			
<i>Initial model used</i>	8VXH (PDB)	AF-P77757-F1 (AlphaFold)	AF-P77757-F1 (AlphaFold)
<i>Map sharpening B factor (Å²)</i>	-89.4	-93.7	-126.2
<i>Residue range (aa)</i>	2-206, 212-319	3-206, 212-319	2-319
Model composition			
<i>Chains</i>	5	4	8
<i>Non-hydrogen atoms</i>	9,902	9,712	10,068
<i>Protein residues</i>	1,252	1,248	1,272
<i>Nucleotide</i>	0	0	4

Water	130	0	0			
Ligands	0	0	MN: 4			
Bonds (RMSD)						
Length (Å) (# > 4s)	0.003 (0)	0.002 (0)	0.003 (0)			
Angles (°) (# > 4s)	0.461 (0)	0.462 (0)	0.483 (0)			
Ramachandran plot						
Outliers (%)	0.00	0.00	0.00			
Allowed (%)	0.32	1.30	2.06			
Favored (%)	99.68	98.70	97.94			
Validation						
MolProbity score	0.81	0.80	0.91			
Clashscore	1.06	1.02	1.53			
Rotamer outliers (%)	0	0	0			
Cβ outliers (%)	0	0	0			
CaBLAM outliers (%)	0.66	0.66	0.96			
EM-Ringer score	5.39	2.76	2.03			
Q-Score	0.75	0.72	0.64			
B-factors (Å²)						
Protein (min/max/mean)	1.04/101.97/35.74	5.10/117.41/48.42	3.19/83.10/54.87			
Nucleotide (min/max/mean)	-	-	45.22/64.19/54.52			
Ligand (min/max/mean)	-	-	83.72/83.72/83.72			
Water (min/max/mean)	11.56/54.00/20.94	-	-			
Resolution Estimates (Å)						
	Masked	Unmasked	Masked	Unmasked	Masked	Unmasked
d FSC (half maps; 0.143)	2.7	2.8	2.8	2.9	3.0	3.1
d 99 (full/half1/half2)	3.0/1.4/1.4	3.0/1.4/1.4	3.1/2.4/2.4	3.0/2.2/2.2	3.2/1.8/1.8	3.2/1.7/1.7
d model	3.0	3.0	3.0	3.0	3.2	3.2
d FSC model (0/0.143/0.5)	2.5/2.6/2.8	2.5/2.7/2.9	2.4/2.6/2.9	2.4/2.7/3.0	2.5/2.7/3.1	2.7/2.9/3.2
Maps						
Map min/max/mean	-0.56/0.73/0.01		-1.40/1.89/0.03		-0.84/1.35/0.02	
Recommended contour level	0.072		0.203		0.103	
Model vs. Data						
CC (mask)	0.86		0.81		0.79	
CC (box)	0.68		0.65		0.61	
CC (peaks)	0.69		0.63		0.59	
CC (volume)	0.81		0.77		0.75	
Mean CC for ligands	0.61		-		0.78	

Supplementary Table 2. Linear DNA fragments and primers used for *arnC* gene cloning.

Name	Sequence
Sen_ArnC_opt_N (1,068bp)	CACGAAAACCTGTATTTTCAATCCTACGTAGGCGGTGGATCTGGCGGTGGATCCATGTTTGAT GCGGCGCCGATTAAAAAAGTGAGCGTGGTGAATCCGGTGTATAACGAACAAGAAAGCCTGCC GGAAGTGAATCGCCGCACCACCACCGCGTGCGAAAGCCTGGGCAAAGCGTGGGAAATTCTG CTGATTGATGATGGCAGCAGCGATAGCAGCGCGGAAGTATGGTGAAGCGAGCCAAGAAGC GGATAGCCATATTATTAGCATTCTGCTGAACCGCAACTATGGTCAGCATGCGGCTATTATGGC GGGCTTTAGCCATGTGAGCGGCGATCTGATTATTACCCTGGATGCGGATCTGCAGAACCCGC CGGAAGAAATTCCGCGCCTGGTGGCGAAAGCGGATGAAGGCTTTGATGTGGTGGGCACCGT GCGTCAGAACCGCCAAGATAGCCTGTTTCGCAAAGCGCGAGCAAAATTATTAACCTGCTGAT TCAGCGCACCACCGGCAAAGCGATGGGCGACTATGGCTGCATGCTGCGCGCGTATCGCCGC CCGATTATTGATACCATGCTGCGCTGCCATGAACGCAGCACCTTTATTCGATTCTGGCGAAC ATTTTTGCGCGCCGCGCGACCGAAATTCGGTGCATCATGCGGAACGGAATTTGGCGATAG CAAATATAGCTTTATGCGCCTGATTAACCTGATGTATGATCTGGTGACCTGCCTGACCACCAC CCGCTGCGCCTGCTGAGCCTGCTGGGCGAGCGTGATTGCGATTGGCGGCTTTAGCCTGAGCG TGCTGCTGATTGTGCTGCGCCTGGCGCTGGGCCCGCAGTGGGCGGCGGAAGGCGTGTTTAT GCTGTTTGGGTGCTGTTTACCTTTATTGGCGCGCAGTTTATTGGCATGGGCTGCTGGGCGA ATATATTGGCCGCATTATAACGATGTGCGCGCGCGCCCGCGCTATTTTGTGCAGCAAGTGAT TTATCCGGAAGACCCCCGTTTACCGAAGAAAGCCATCAGTAAGTATAATATTGAGGGAAGTC GAGCACCACC
Sen_ArnC_opt_C (1,065bp)	CCCCTCTAGACCTTAAGAAGGAGATATACTATGTTTGATGCGGCGCCGATTAAAAAAGTGAGC GTGGTGATTCCGGTGTATAACGAACAAGAAAGCCTGCCGGAAGTATTCCGCCGACCACCAC CGCGTGCGAAAGCCTGGGCAAAGCGTGGGAAATTCTGCTGATTGATGATGGCAGCAGCGATA GCAGCGCGAACTGATGGTGAAAGCGAGCCAAGAAGCGGATAGCCATATTATTAGCATTCTG CTGAACCGCAACTATGGTCAGCATGCGGCTATTATGGCGGGCTTTAGCCATGTGAGCGGCGA TCTGATTATTACCCTGGATGCGGATCTGCAGAACCCGCCGAAGAAATTCGCGCCTGGTGG CGAAAGCGGATGAAGGCTTTGATGTGGTGGGCACCGTGCCTCAGAACCGCCAAGATAGCCTG TTTCGCAAAGCGCGAGCAAAATTATTAACCTGCTGATTCAGCGCACCACCGCAAAGCGATG GGCGACTATGGCTGCATGCTGCGCGCGTATCGCCGCCCGATTATTGATACCATGCTGCGCTG CCATGAACGCAGCACCTTTATTCCGATTCTGGCGAACATTTTTGCGCGCCGCGCGACCGAAAT TCCGGTGCATCATGCGGAACGCGAATTTGGCGATAGCAAATATAGCTTTATGCGCCTGATTAA CCTGATGTATGATCTGGTGACCTGCCTGACCACCACCCCGCTGCGCCTGCTGAGCCTGCTGG GCAGCGTGATTGCGATTGGCGGCTTTAGCCTGAGCGTGCTGCTGATTGTGCTGCGCCTGGCG CTGGGCCCGCAGTGGGCGGCGGAAGGCGTGTTTATGCTGTTTGGGTGCTGTTTACCTTTAT TGCGCGCAGTTTATTGGCATGGGCTGCTGGGCGAATATATTGGCCGCAATTATAACGATGT GCGCGCGCGCCGCGCTATTTTGTGCAGCAAGTGATTTATCCGGAAGACCCCCGTTTACCG AAGAAAGCCATCAGGGCGGTGGATCTGGCGGTGGATCCGCCGAAAACCTCTATTTTCAGGGA CATCAT
Kpn_ArnC_opt_N (1,068bp)	CACGAAAACCTGTATTTTCAATCCTACGTAGGCGGTGGATCTGGCGGTGGATCCATGCTGACC TATCCGCGCGGTGAAAAAAGTGAGCGTGGTGAATCCGGTGTATAACGAACAAGATAGCCTGCC GGAAGTGTGCGCCGCACCGATGTGGCGTGCGCGACCTGGGCCGTGAGTATGAAATTCTG CTGATTGATGATGGCAGCAGCGATGATAGCGCGCGCATGCTGACCGAAGCGGCGGAAGCGG AAGGCAGCCATGTGGTGGCGGTGCTGCTGAACCGCAACTATGGTCAGCATAGCGCGATTATG GCGGGCTTTAGCCATGTGACCGGCGATCTGATTATTACCCTGGATGCGGATCTGCAGAACCC GCCGGAAGAAATTCGCGCCTGGTGGCGAAAGCGGATGAAGGCTATGATGTGGTGGGCACC GTGCGTCAGAACCGCCAAGATAGCATTTTTCGCAAGACAGCGTCGAAGATGATAAACCCGCT GATTCAGCGCACCAACCGCAAAGCGATGGGCGATTATGGCTGCATGCTGCGCGCGTATCGC CGCCATATTATTGATGCGATGCTGAACCTGCCATGAACGCAGCACCTTTATTCGATTCTGGCG AACACCTTTGCGCGCCGCGCGGTGGAATTCGGTGTATGCATGCGGAACGCGAATTTGGCGA TAGCAAATATAGCTTTATGCGCCTGATTAACCTGATGTATGATCTGGTGACCTGCCTGACCACC ACCCCGCTGCGCCTGCTGAGCATTTTTGGCAGCGTGATTGCGCTGCTGGGCTTTGCGTTTTGG CCTGCTGCTGGTGGTGTGCGCCTGGCGTTTGGCCCGCAGTGGGCGGCGGAAGGCGTGTTT ATGCTGTTTGGGTGCTGTTTATGTTTATTGGCGCGCAGTTTGTGGGCATGGGCTGCTGGGC GAATATATTGGCCGCATTATAACGATGTGCGCGCGCGCCCGCGCTATTTTATTCAGCGCGTG GTGCGTCAGCCGGAACCGCGTCGAAGGAGGAGGATCGCAGCTAAGTATAATATTGAGGGAA CTCGAGCACCACC
Kpn_ArnC_opt_C (1,065bp)	CCCCTCTAGACCTTAAGAAGGAGATATACTATGCTGACCTATCCGCCGGTGAAAAAAGTGAGC GTGGTGATTCCGGTGTATAACGAACAAGATAGCCTGCCGGAAGTGTGCGCCGCACCGATGT GGCGTGCGCGACCCCTGGGCCGTGAGTATGAAATTCTGCTGATTGATGATGGCAGCAGCGATG ATAGCGCGCGCATGCTGACCGAAGCGGCGGAAGCGGATGATGGTGGCGGTGCT

	GCTGAACCGCAACTATGGTCAGCATAGCGCGATTATGGCGGGCTTTAGCCATGTGACCGGCG ATCTGATTATTACCCTGGATGCGGATCTGCAGAACCCGCCGGAAGAAATTCGCGCCTGGTG GCGAAAGCGGATGAAGGCTATGATGTGGTGGGCACCGTGCGTCAGAACCGCCAAGATAGCAT TTTTCGCAAGACAGCGTCGAAGATGATAAACCGCCTGATTACGCGCACCAACCGGCAAAGCGA TGGGCGATTATGGCTGCATGCTGCGCGCGTATCGCCGCCATATTATTGATGCGATGCTGAACT GCCATGAACGCAGCACCTTTATTCCGATTCTGGCGAACACCTTTGCGCGCCGCGCGGTGGAA ATTCCGGTGATGCATGCGGAACGCGAATTTGGCGATAGCAAATATAGCTTTATGCGCCTGATT AACCTGATGTATGATCTGGTGACCTGCCTGACCACCACCCCGCTGCGCCTGCTGAGCATTTTT GGCAGCGTGATTGCGCTGCTGGGCTTTGCGTTTGGCCTGCTGCTGGTGGTGCTGCGCCTGG CGTTTGGCCCCGAGTGGGCGGCGGAAGGCGTGTATGCTGTTTGGCGGTGCTGTTTATGTTT ATTGGCGCGCAGTTTTGTGGGCATGGCCTGCTGGGCGAATATATTGGCCGATTATATAACGAT GTGCGCGCGCGCCCGCGCTATTTTATTACGCGCGTGGTGCGTCAGCCGAAACCGCGTCTGA AGGAGGAGGATCGCAGCGGCGGTGGATCTGGCGGTGGATCCGCCGAAAACCTCTATTTTCA GGGACATCAT
Eco_ArnC_opt_N (1,053bp)	CACGAAAACCTGTATTTTCAATCCTACGTAGGCGGTGGATCTGGCGGTGGATCCATGTTTGAA ATTCATCCGGTGAAAAAAGTGAGCGTGGTGATTCCGGTGATAACGAACAAGAAAGCCTGCCG GAACTGATTGCCGCGACCAACCGCGTGCGAAAGCCTGGGCAAAGAATATGAAATTCTGCT GATTGATGATGGCAGCAGCGATAACAGCGCGCATATGCTGGTGGAAGCGAGCCAAGCGGAAA ACAGCCATATTGTGAGCATTCTGCTGAACCGCAACTATGGTCAGCATAGCGCGATTATGGCGG GCTTTAGCCATGTGACCGGCGATCTGATTATTACCCTGGATGCGGATCTGCAGAACCCGCCG GAAGAAATTCGCGCCTGGTGGCGAAAGCGGATGAAGGCTATGATGTGGTGGCACCCTGCG GTGAGAACCGCCAAGATAGCTGGTTTCGCAAAACCGCGAGCAAAATGATTAACCGCCTGATT AGCGCACCAACCGGCAAAGCGATGGGCGATTATGGCTGCATGCTGCGCGCGTATCGCCGCCA TATTGTGGATGCGATGCTGCATTGCCATGAACGCAGCACCTTTATTCCGATTCTGGCGAACAT TTTTGCGCGCCGCGCGATTGAAATTCCGGTGCATCATGCGGAACGCGAATTTGGCGAAAGCA AATATAGCTTTATGCGCCTGATTAACCTGATGTATGATCTGGTGACCTGCCTGACCACCACCC CGCTGCGCATGCTGAGCCTGCTGGGCAGCATTATTGCGATTGGCGGCTTTAGCATTGCGGTG CTGCTGGTGATTCTGCGCCTGACCTTTGGCCCGCAGTGGGCGGCGGAAGGCGTGTATGCT GTTTGGCGGTGCTGTTTACCTTTATTGGCGCGCAGTTTATTGGCATGGGCCTGCTGGGCGAATA TATTGGCCGCATTTATACCGATGTGCGCGCGCGCCCGCGCTATTTTGTGCAGCAAGTGATTG CCCGAGCAGCAAAGAAAACGAATAAGTATAATATTGAGGGAACTCGAGCACCACC
Eco_ArnC_opt_C (1,050bp)	CCCCTCTAGACCTTAAGAAGGAGATATACTATGTTTGAAATTCATCCGGTGAAAAAAGTGAGC GTGGTGATTCCGGTGATAACGAACAAGAAAGCCTGCCGGAAGTATTCGCCGCAACCACCAC CGCGTGCGAAAGCCTGGGCAAAGAATATGAAATTCTGCTGATTGATGATGGCAGCAGCGATA ACAGCGCGCATATGCTGGTGGAAGCGAGCCAAGCGGAAAAACAGCCATATTGTGAGCATTCTG CTGAACCGCAACTATGGTCAGCATAGCGCGATTATGGCGGGCTTTAGCCATGTGACCGGCGA TCTGATTATTACCCTGGATGCGGATCTGCAGAACCCGCCGGAAGAAATTCGCGCCTGGTGG CGAAAGCGGATGAAGGCTATGATGTGGTGGGCACCGTGCGTCAGAACCGCCAAGATAGCTG GTTTCGCAAAACCGCGAGCAAAATGATTAACCGCCTGATTACGCGCACCAACCGGCAAAGCGA TGGGCGATTATGGCTGCATGCTGCGCGCGTATCGCCGCCATATTGTGGATGCGATGCTGCAT TGCCATGAACGCAGCACCTTTATTCCGATTCTGGCGAACATTTTTGCGCGCCGCGCGATTGAA ATTCCGGTGATCATGCGGAACGCGAATTTGGCGAAAGCAAATATAGCTTTATGCGCCTGATT AACCTGATGTATGATCTGGTGACCTGCCTGACCACCACCCCGCTGCGCATGCTGAGCCTGCT GGGCAGCATTATTGCGATTGGCGGCTTTAGCATTGCGGTGCTGCTGGTGATTCTGCGCCTGA CCTTTGGCCCGCAGTGGGCGGCGGAAGGCGTGTATGCTGTTTGGCGGTGCTGTTTACCTTT ATTGGCGCGCAGTTTATTGGCATGGGCCTGCTGGGCGAATATATTGGCCGCATTTATACCGAT GTGCGCGCGCGCCCGCGCTATTTTGTGCAGCAAGTGATTGCCCCGAGCAGCAAAGAAAACGA AGGCGGTGGATCTGGCGGTGGATCCGCCGAAAACCTCTATTTTCAGGGACATCAT
pNYCOMPS-N_3LIC_F (29bp)	GTATAATATTGAGGGAACCTCGAGCACCAC
pNYCOMPS- N_5LIC_R (33bp)	TACGTAGGATTGAAAATACAGGTTTTTCGTGATG
pNYCOMPS- Cterm_3LIC_F (28bp)	GCCGAAAACCTCTATTTTCAGGGACATC
pNYCOMPS- Cterm_5LIC_R (31bp)	AGTATATCTCCTTCTTAAGGTCTAGAGGGGA

Supplementary Table 3. MD simulation summary

System	Sim. Type	Ligands	# Water	# POPE	# POPG	# CARD	# Na ⁺	# Cl ⁻
ArnC	CG	-	7338	253	72	35	152	10
ArnC + 18 UndP	CG	UndP	7355	230	65	32	161	-
ArnC + 32 UndP	AT	UndP	29420	230	65	32	161	-
State1	AT	UndP/UDPA/Mg ²⁺	72094	626	152	-	279	117
State2	AT	UndP/UDPA/ Mg ²⁺	72094	626	152	-	279	117
State3	AT	UndP/UDPA/ Mg ²⁺	72094	626	152	-	279	117